ECE 796:

Models of the Neuron

Slides for Lecture #9

Friday, March 23, 2007

Kinetic model of sodium channel

$$
\begin{array}{ccccccc}
m_0h_0 & \underset{\beta_m}{\overset{3\alpha_m}{\rightleftharpoons}} & m_1h_0 & \underset{2\beta_m}{\overset{2\alpha_m}{\rightleftharpoons}} & m_2h_0 & \underset{3\beta_m}{\overset{\alpha_m}{\rightleftharpoons}} & m_3h_0 \\
\alpha_h \Big\Downarrow \beta_h & & \alpha_h \Big\Downarrow \beta_h & & \alpha_h \Big\Downarrow \beta_h & & \alpha_h \Big\Downarrow \beta_h \\
m_0h_1 & \underset{\beta_m}{\overset{3\alpha_m}{\rightleftharpoons}} & m_1h_1 & \underset{2\beta_m}{\overset{2\alpha_m}{\rightleftharpoons}} & m_2h_1 & \underset{3\beta_m}{\overset{\alpha_m}{\rightleftharpoons}} & m_3h_1
\end{array}
$$

The number of channels in the state m_3h_1 determines the sodium conductance.

Kinetic model of potassium channel

$$n_0 \underset{\beta_n}{\overset{4\alpha_n}{\rightleftharpoons}} n_1 \underset{2\beta_n}{\overset{3\alpha_n}{\rightleftharpoons}} n_2 \underset{3\beta_n}{\overset{2\alpha_n}{\rightleftharpoons}} n_3 \underset{4\beta_n}{\overset{\alpha_n}{\rightleftharpoons}} n_4$$

The number of channels in the state n_4 determines the potassium conductance.

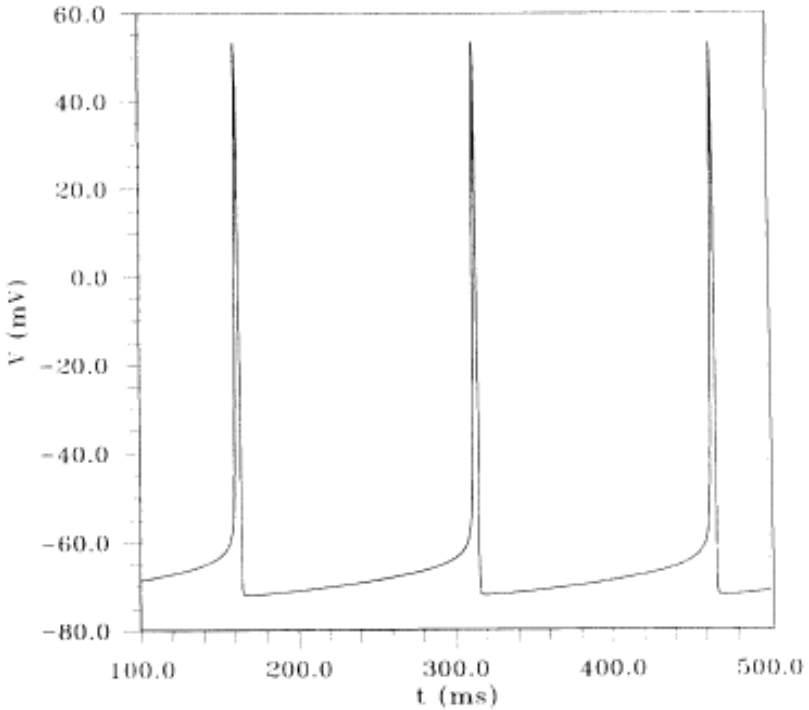

FIG. 4. Figures 4–11 are for $N_{Na}=300$, $N_K=30$, $C=1$ $\mu F/cm^2$, and $A=1$ μm^2 with a time step of 5 μsec. The initial conditions are the unstable steady-state values. This figure is the voltage for the Hodgkin-Huxley model.

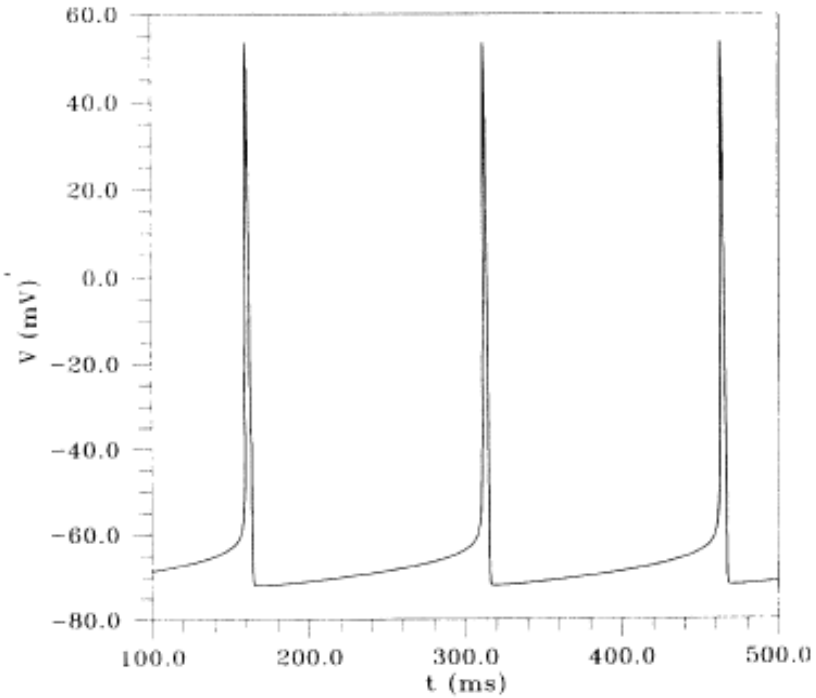

FIG. 5. This figure is the voltage for the modified Hodgkin-Huxley model.

(from Fox & Lu, 1994)

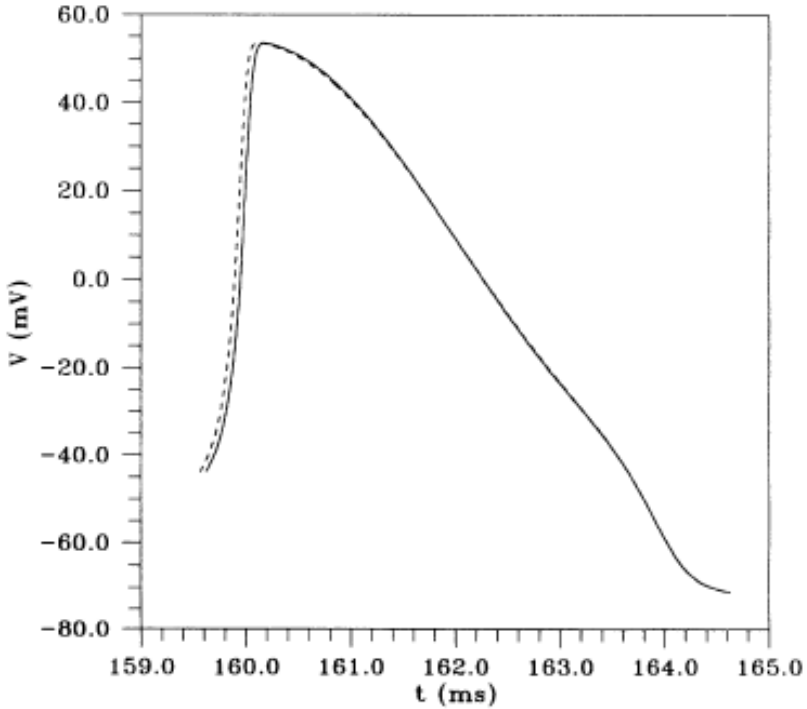

FIG. 10. This is a direct comparison of the voltage for the two models with the time axis expanded about 100-fold compared with Figs. 4 and 5. The dashed curve is for the Hodgkin-Huxley model and the solid curve is for the modified Hodgkin-Huxley model.

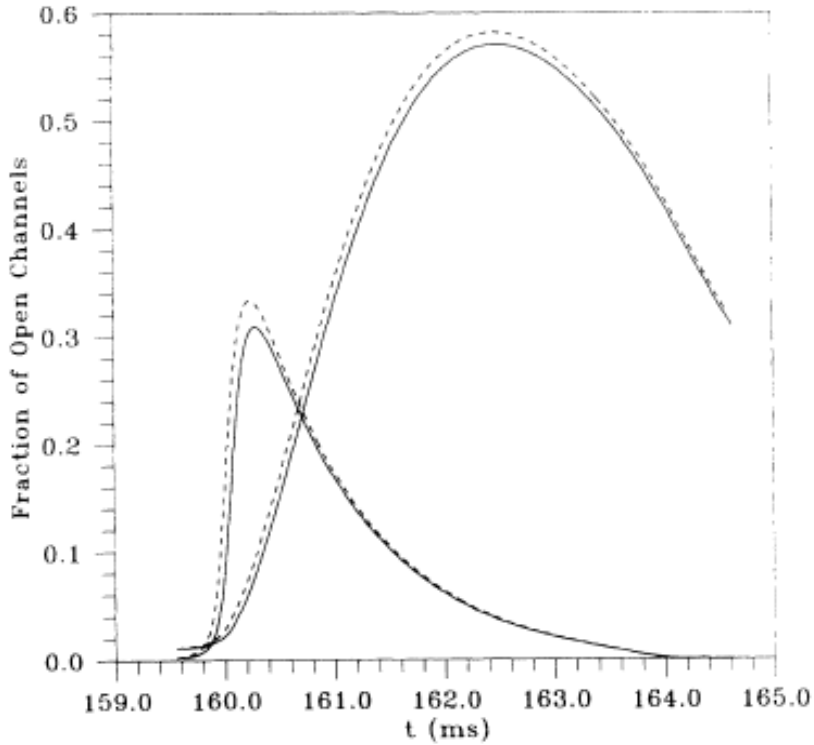

FIG. 11. This a direct comparison of n^4 with x_4, and of m^3h with y_{31}, with the time axis expanded about 100-fold compared with Figs. 6, 7, 8, and 9. The dashed curve is for the Hodgkin-Huxley model and the solid curve is for the modified Hodgkin-Huxley model. The higher pair of curves are for potassium.

(from Fox & Lu, 1994)

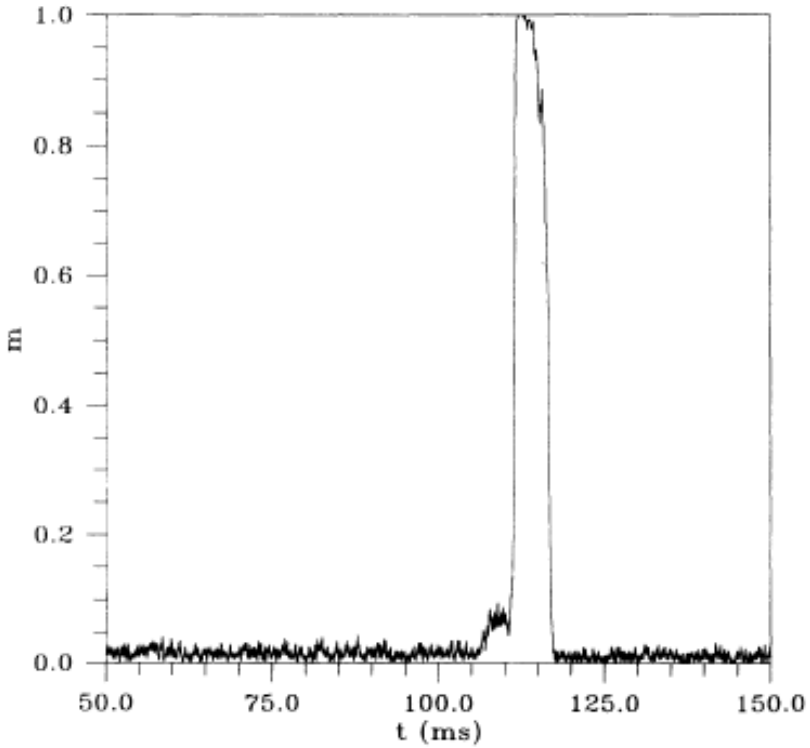

FIG. 16. This shows variable m determined from the master equations. To get m from the master-equation simulation, one counts the total number of first m elements (out of three) in each channel that are open and divides by N_{Na}.

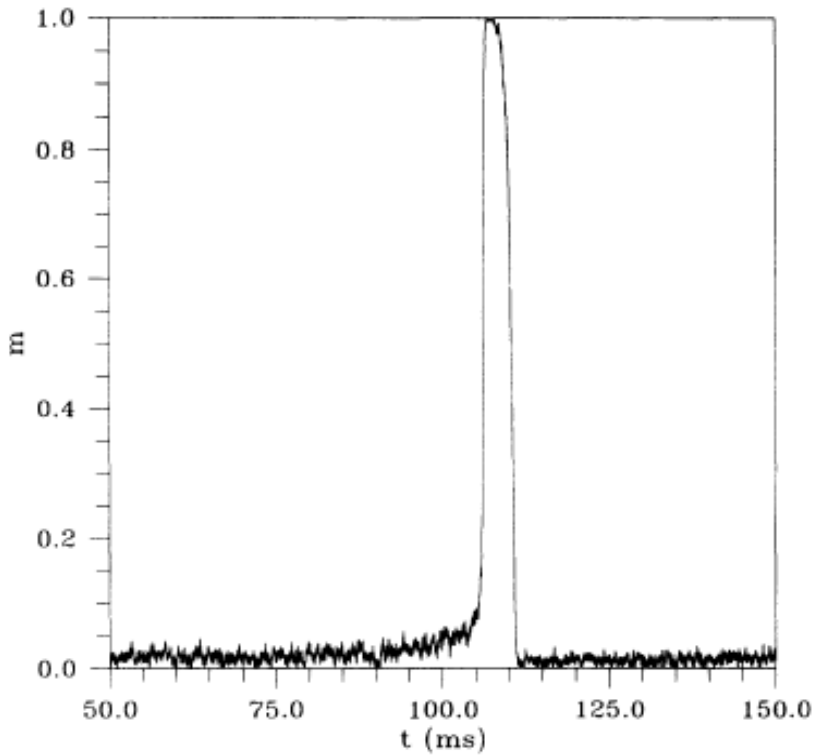

FIG. 17. This shows variable m determined from the stochastic Hodgkin-Huxley model.

(from Fox & Lu, 1994)

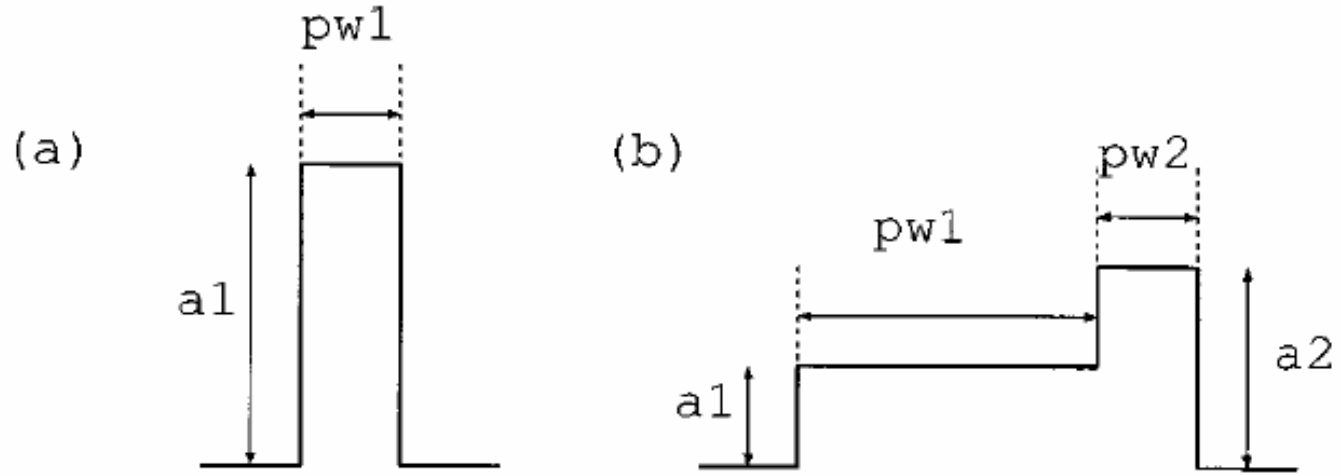

FIGURE 1. Stimulus wave form: monophasic in (a) where a_1 and pw_1, respectively, denote the stimulus current intensity and duration, and preconditioned monophasic in (b), where a_1, pw_1, a_2, and pw_2 stand for the preconditioned current intensity and duration, and the suprathreshold current intensity and duration.

(from Mino et al., 2002)

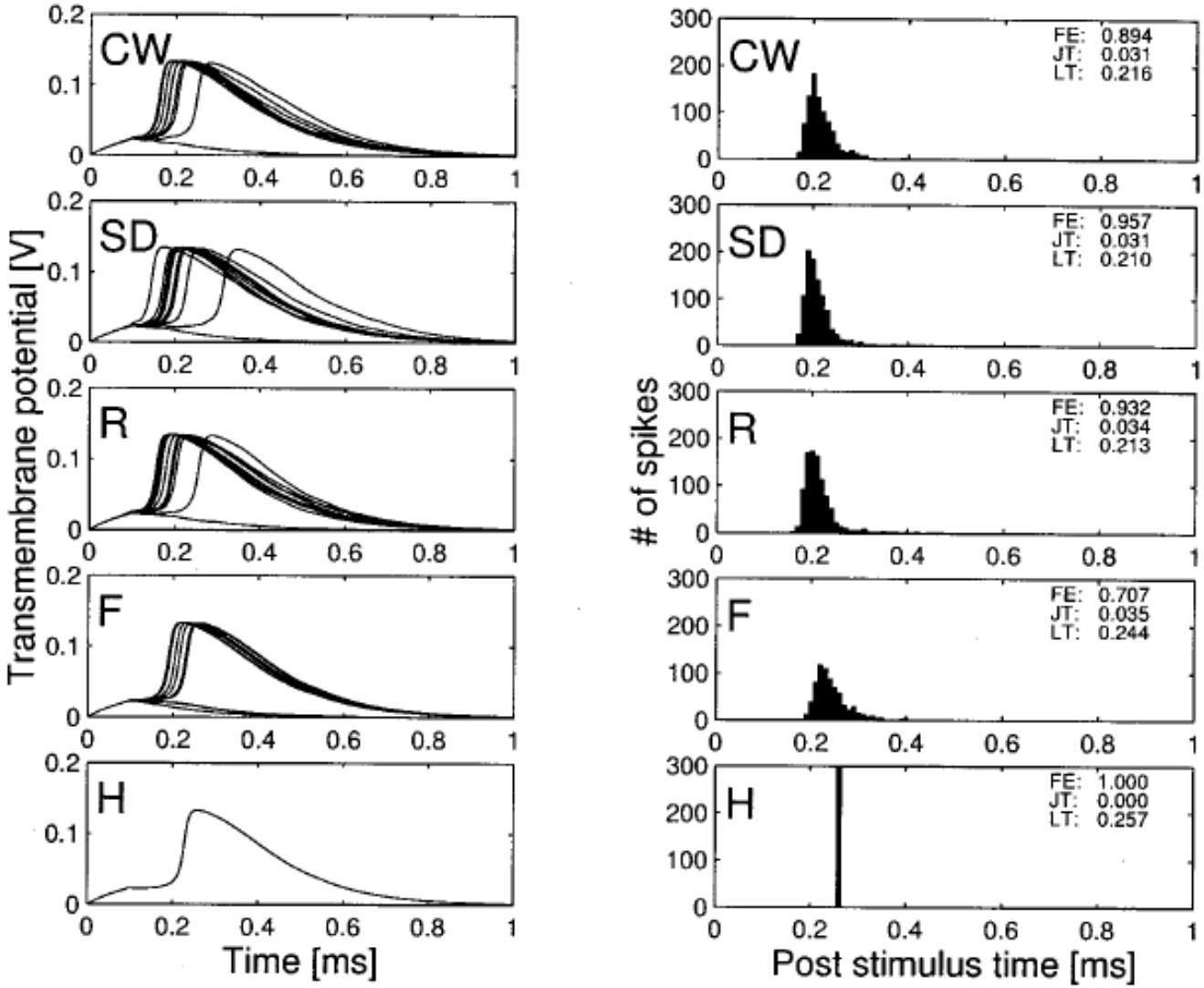

FIGURE 2. Transmembrane potentials in response to ten identical monophasic stimulus pulses with an amplitude of 6.2 pA and a duration of 100 μs (left) and poststimulus time histograms generated from 1000 Monte Carlo runs (right), where FE, JT, and LT are shown in each inset. The sampling step was set at 1 μs.

(from Mino et al., 2002)

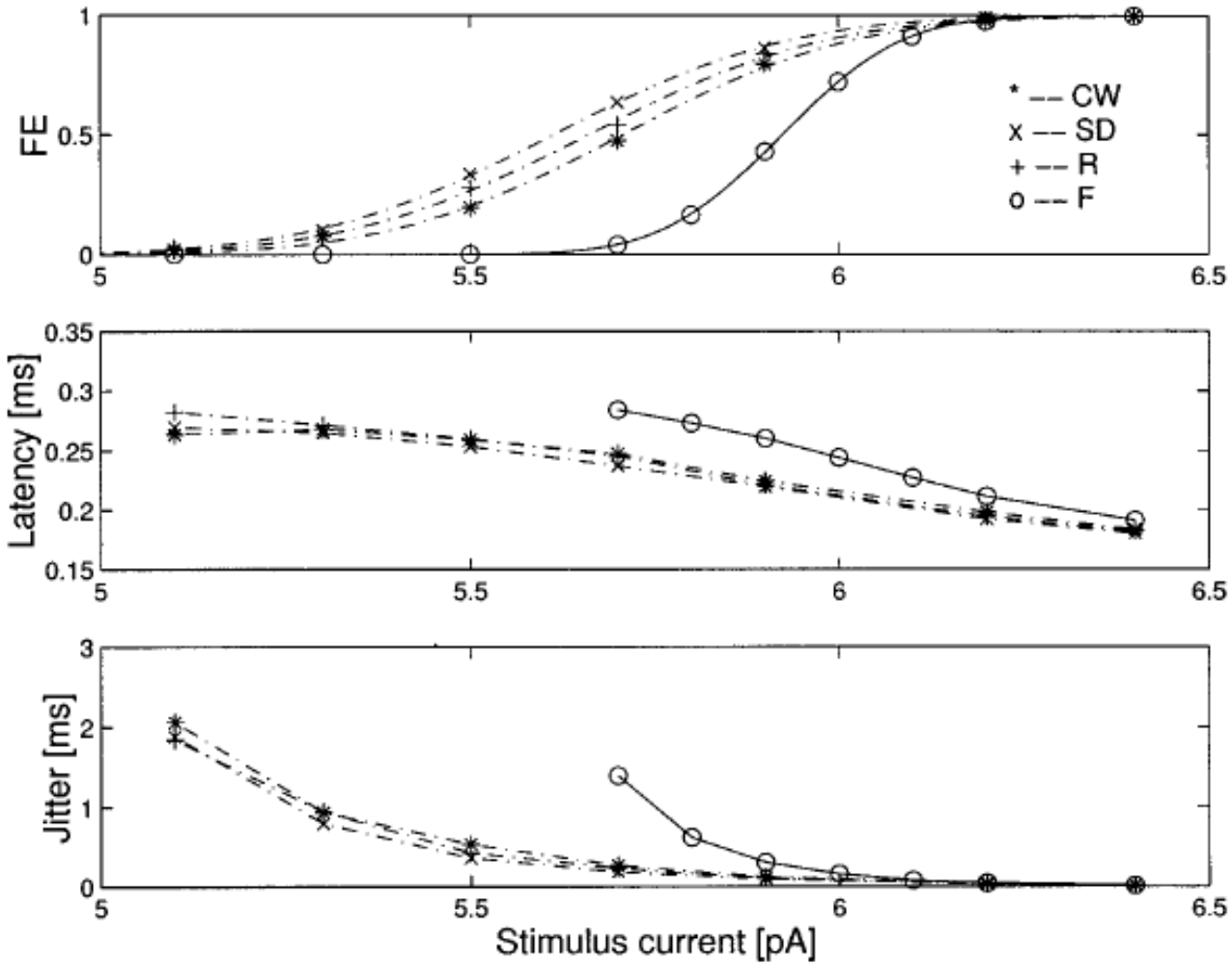

FIGURE 3. FE (top), latency (middle), and jitter (bottom) as a function of stimulus current intensity for four algorithms at $\Delta t = 1\ \mu s$. Stimulus duration was 100 μs. From the data shown in the top panel, I_{th} and RS were estimated for four algorithms: $I_{th} = 5.658$ pA and RS = 0.0350 (CW), $I_{th} = 5.610$ pA and RS = 0.0441 (SD), $I_{th} = 5.657$ pA and RS = 0.0436 (R), and $I_{th} = 5.931$ pA and RS = 0.0215 (F).

(from Mino et al., 2002)

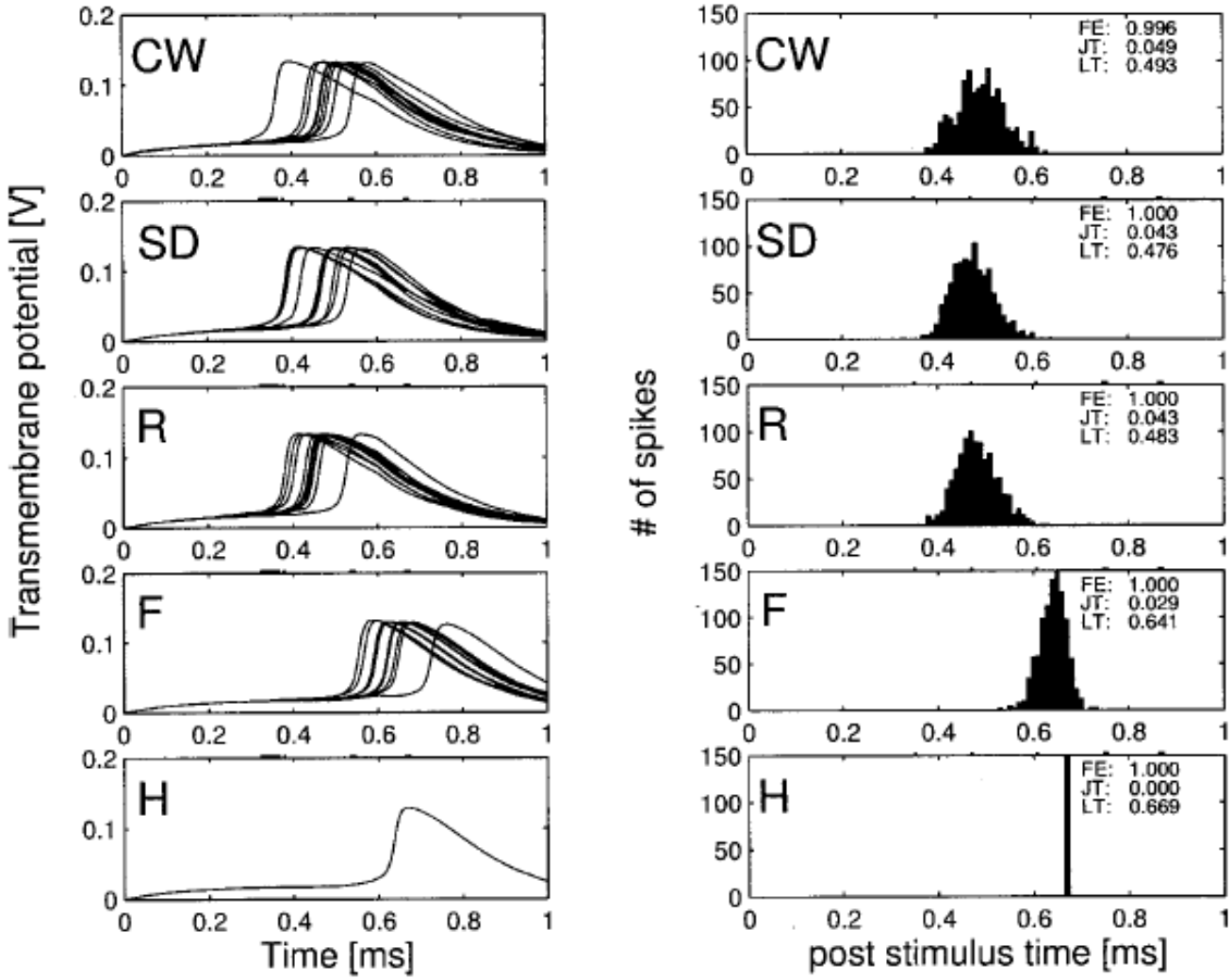

FIGURE 4. Transmembrane potentials in response to ten identical stimulus pulses conditioned (left) at $\Delta t = 1\ \mu$s. Poststimulus time histograms given from 1000 Monte Carlo runs (right). The subthreshold stimulus current of 2.5 pA was applied initially for a duration of 500 μs, followed by a stimulus with an amplitude of 3.5 pA and a duration of 100 μs.

(from Mino et al., 2002)

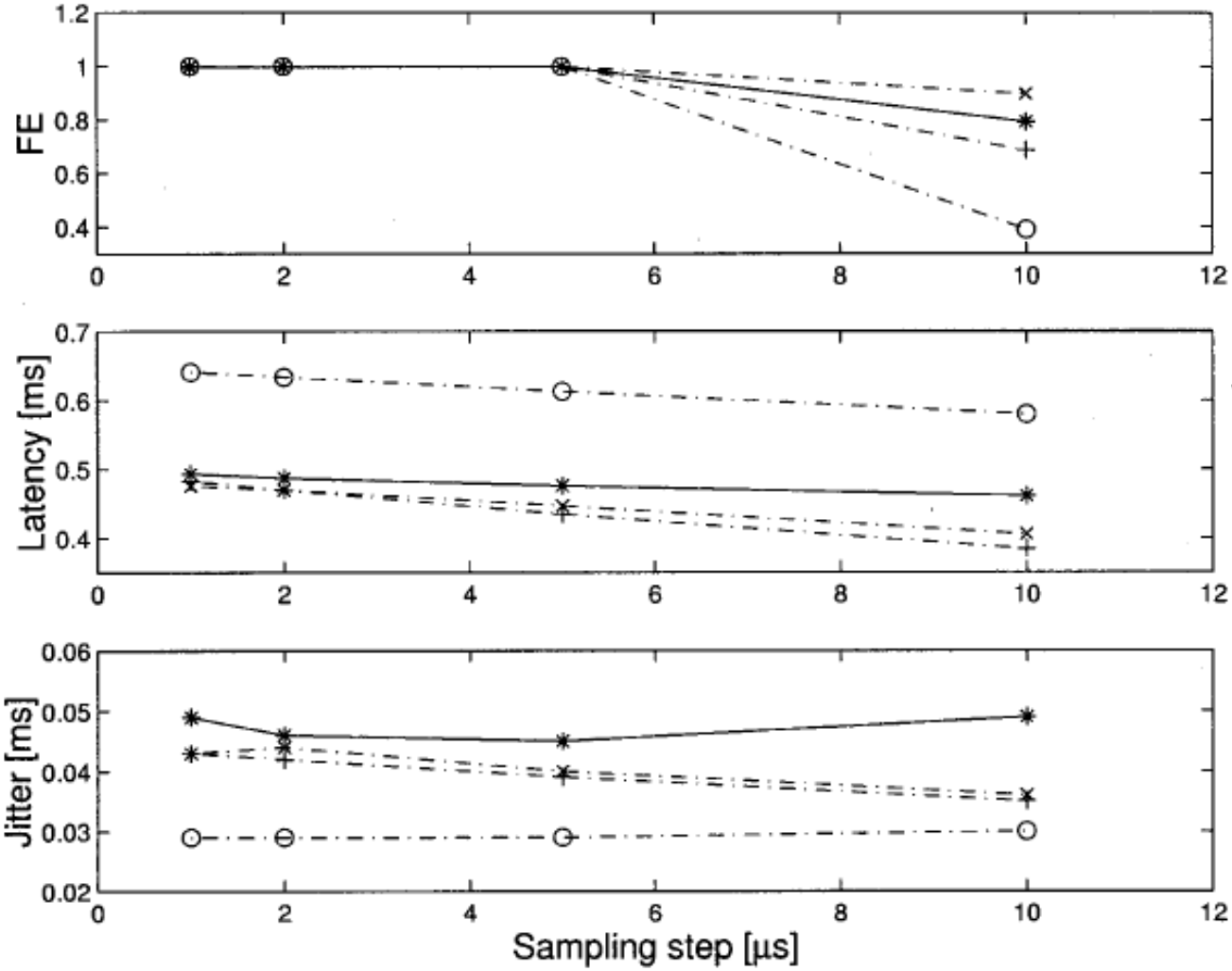

FIGURE 7. FE, latency, jitter vs. the sampling step [1, 2, 5, and 10 (μs)]. Those statistical parameters at each sampling step were estimated from 1000 Monte Carlo runs in which the preconditioned stimuli were presented. The data of CW, SD, R, and F algorithms are, respectively, plotted by the marks $*$, $\times$, $+$, and $\circ$.

(from Mino et al., 2002)

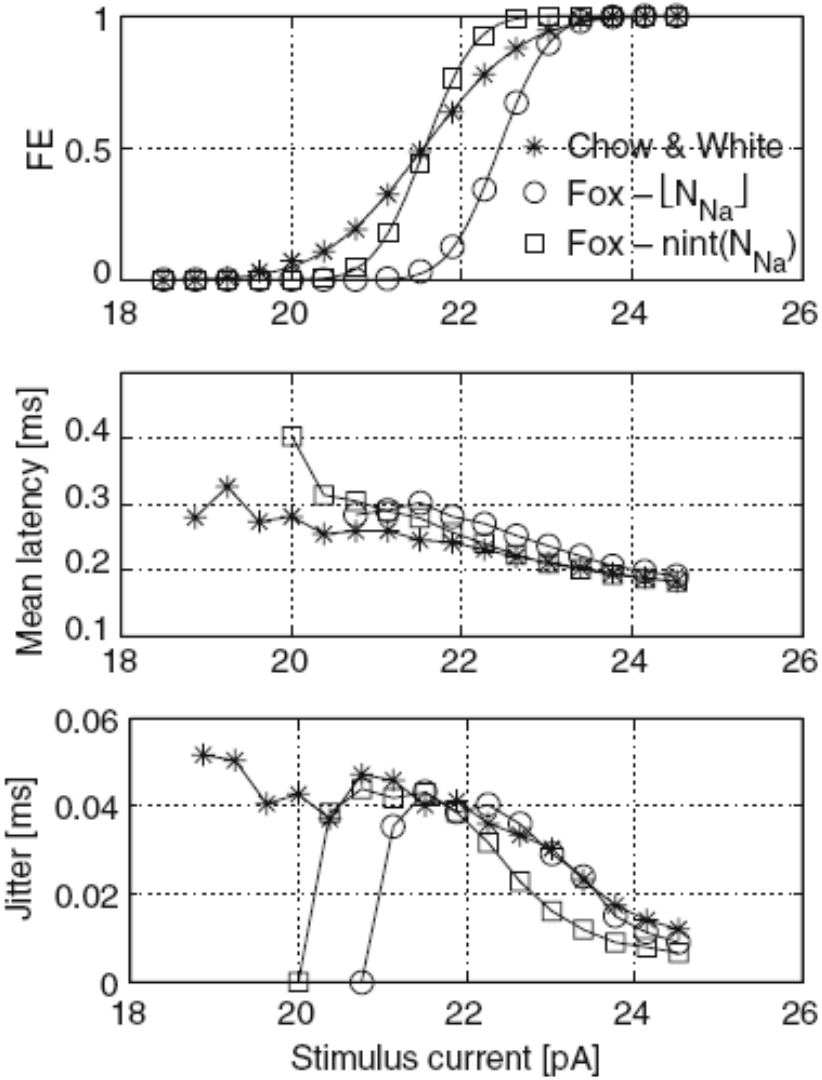

FIGURE 1. Firing efficiency (top), mean latency (middle) and jitter (bottom) versus stimulus current for a monophasic pulse of duration 100 μs for three different algorithms: the Chow & White algorithm (*), the Fox algorithm with rounding down of $N_{Na}(t)$ (○), and the Fox algorithm with rounding of $N_{Na}(t)$ to the nearest integer (□).

(from Bruce, *ABME* 2007)

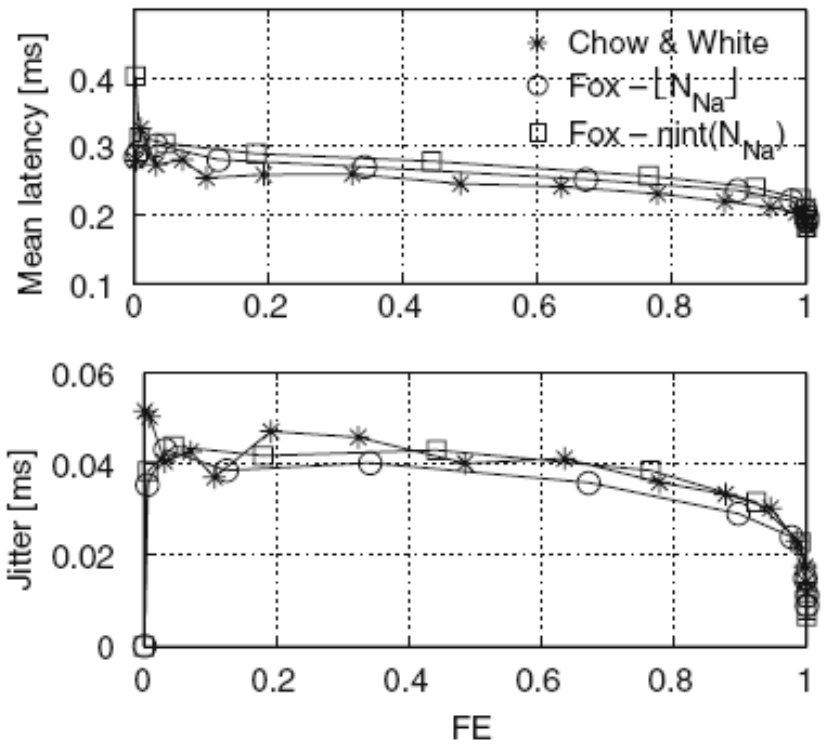

FIGURE 2. Mean latency (top) and jitter (bottom) versus firing efficiency for a monophasic pulse of duration 100 μs for three different algorithms: the Chow & White algorithm (*), the Fox algorithm with rounding down of $N_{Na}(t)$ (○), and the Fox algorithm with rounding of $N_{Na}(t)$ to the nearest integer (□).

(from Bruce, *ABME* 2007)

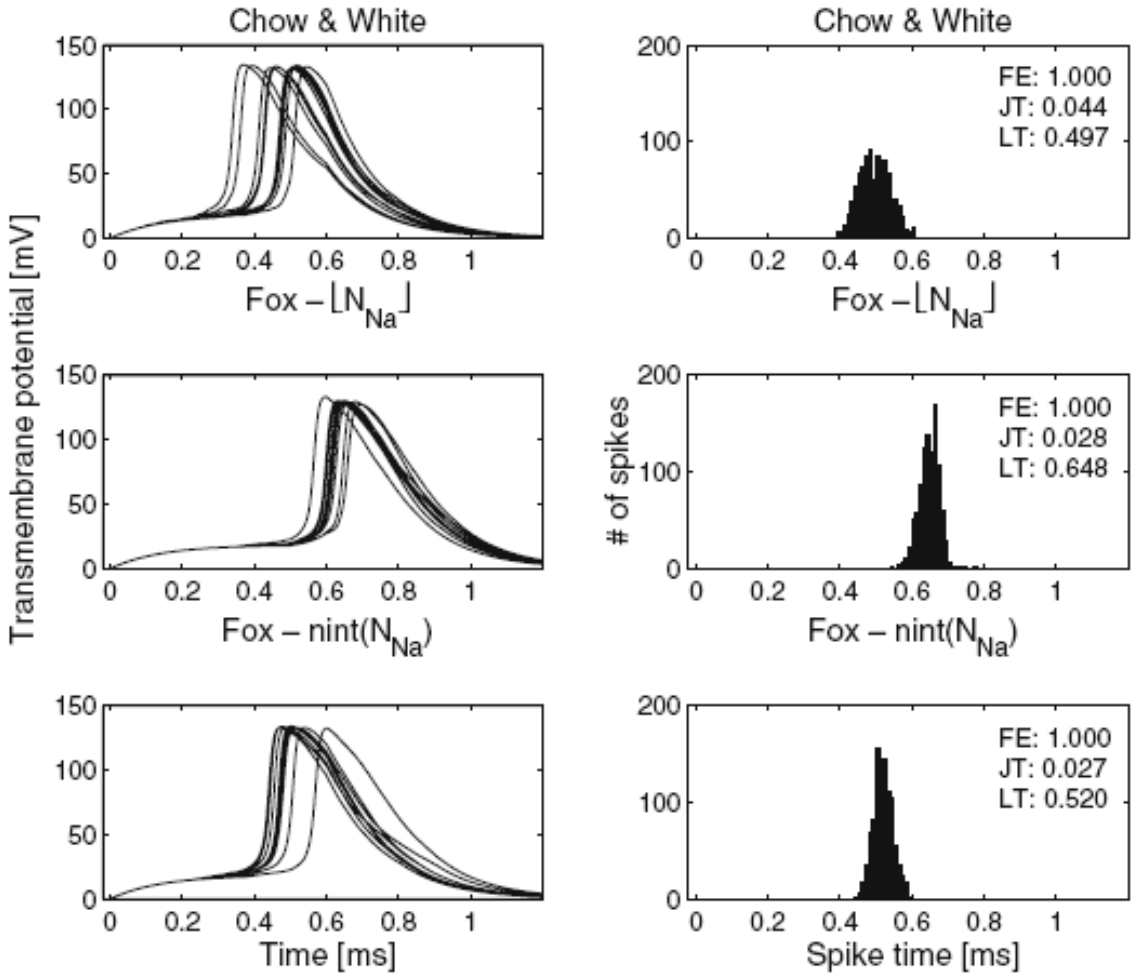

(from Bruce, *ABME* 2007)

FIGURE 3. Example transmembrane potentials in response to 10 identical preconditioned monophasic pulse stimuli (left). Histograms of spike times for 1,000 trials (right). The insets to the histograms give the respective firing efficiency (FE), jitter (JT) and mean latency (LT) for the 1,000 trials. A preconditioning current of 9.434 pA was applied for 500 μs, followed immediately by a current of 13.208 pA for 100 μs.

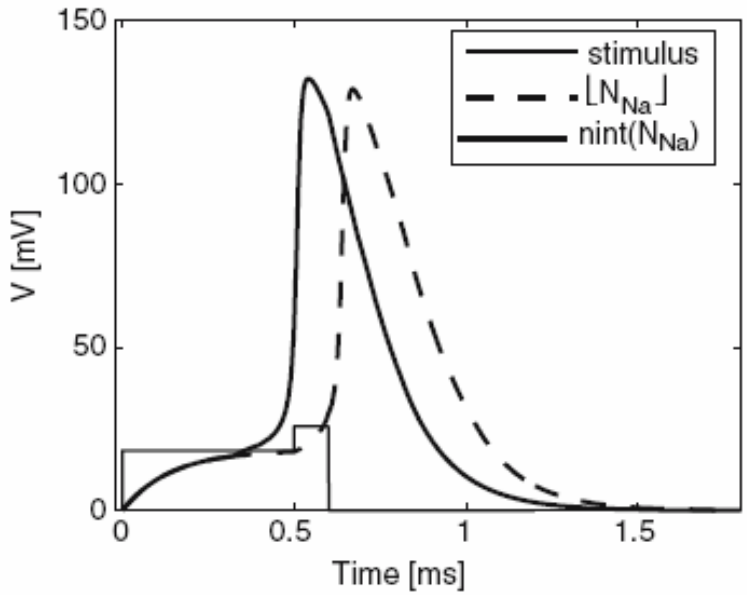

FIGURE 4. Transmembrane potentials from the deterministic equivalent to the Fox model in response to the preconditioned monophasic pulse stimuli.

(from Bruce, *ABME* 2007)

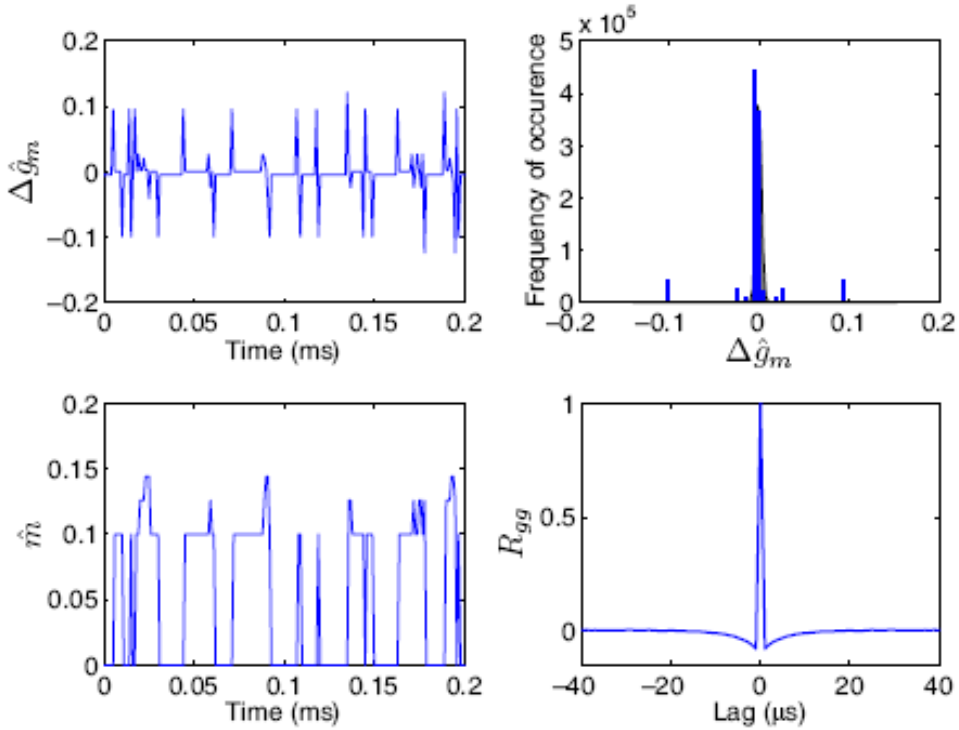

(from Bruce, *IEEE NE* 2007)

Fig. 1. Activation dynamics for 1,000 sodium channels: analysis of m-particle dynamics for relative transmembrane potential $V = 16$ mV. Top left panel: Example time series of $\Delta\hat{g}_m$. Top right panel: Histogram of values of $\Delta\hat{g}_m$. The theoretical distribution derived by Fox and colleagues [1], [2] is shown by the grey-filled Gaussian curve. Bottom left panel: Time series of $\hat{m}$ corresponding to top left panel. Bottom right panel: Autocorrelation function for $\Delta\hat{g}_m$.

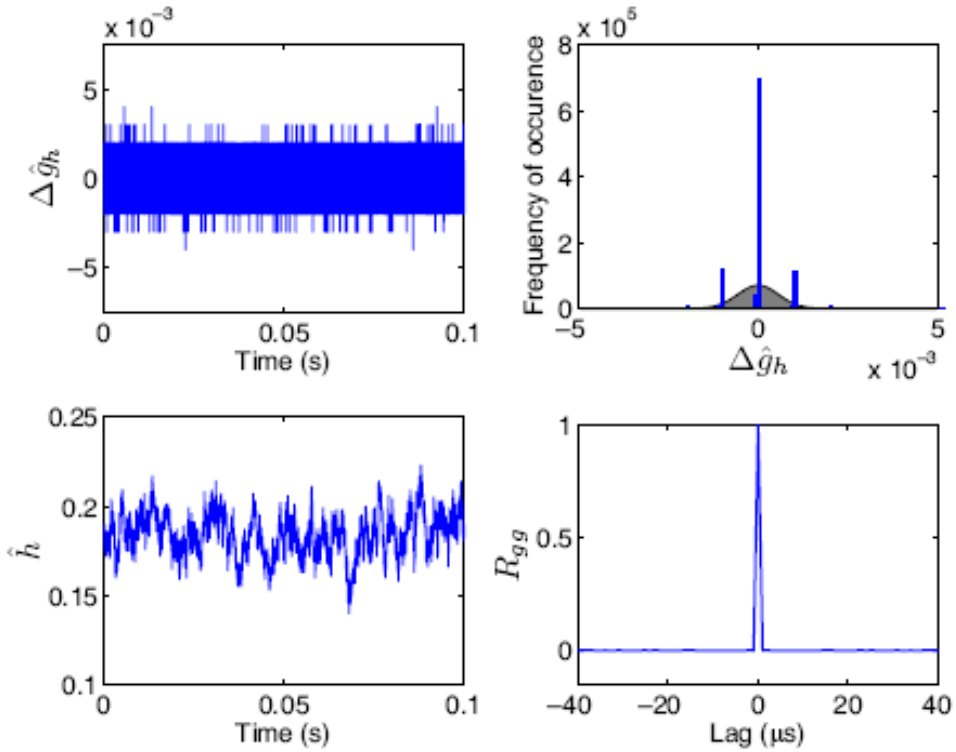

(from Bruce, *IEEE NE* 2007)

Fig. 2. Inactivation dynamics for 1,000 sodium channels: analysis of h-particle dynamics for relative transmembrane potential $V = 16$ mV. Top left panel: Example time series of $\Delta\hat{g}_h$. Top right panel: Histogram of values of $\Delta\hat{g}_h$. The theoretical distribution derived by Fox and colleagues [1], [2] is shown by the grey-filled Gaussian curve. Bottom left panel: Time series of $\hat{h}$ corresponding to top left panel. Bottom right panel: Autocorrelation function for $\Delta\hat{g}_h$.

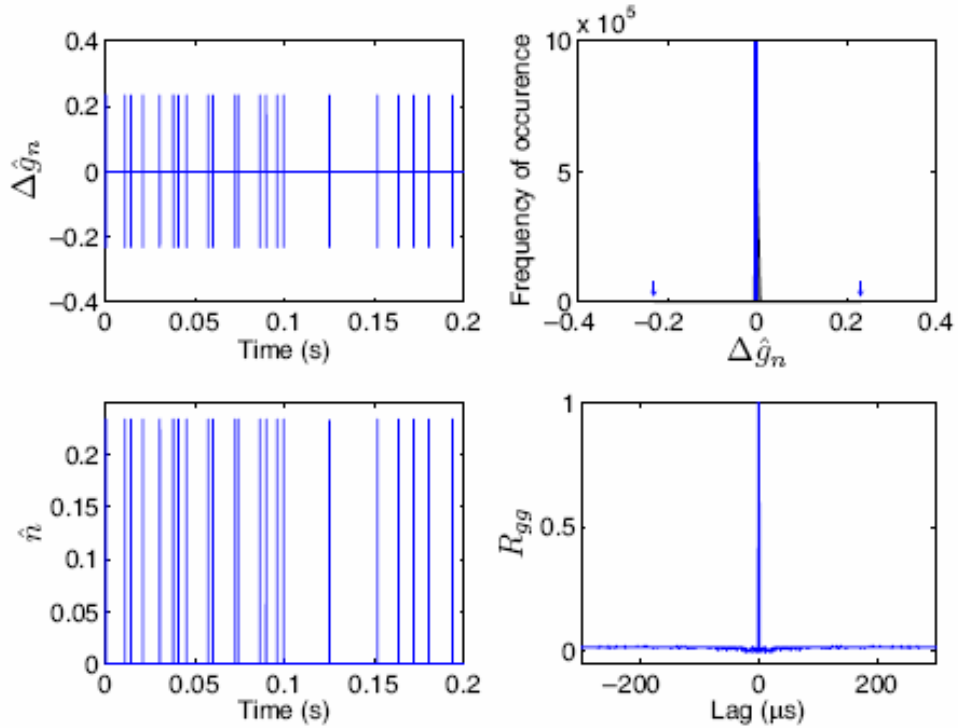

(from Bruce, *IEEE NE* 2007)

Fig. 3. Activation dynamics for 333 potassium channels: analysis of n-particle dynamics for relative transmembrane potential $V = 16$ mV. Top left panel: Example time series of $\Delta\hat{g}_n$. Top right panel: Histogram of values of $\Delta\hat{g}_n$. The theoretical distribution derived by Fox and colleagues [1], [2] is shown by the grey-filled Gaussian curve. Bottom left panel: Time series of $\hat{n}$ corresponding to top left panel. Bottom right panel: Autocorrelation function for $\Delta\hat{g}_n$.

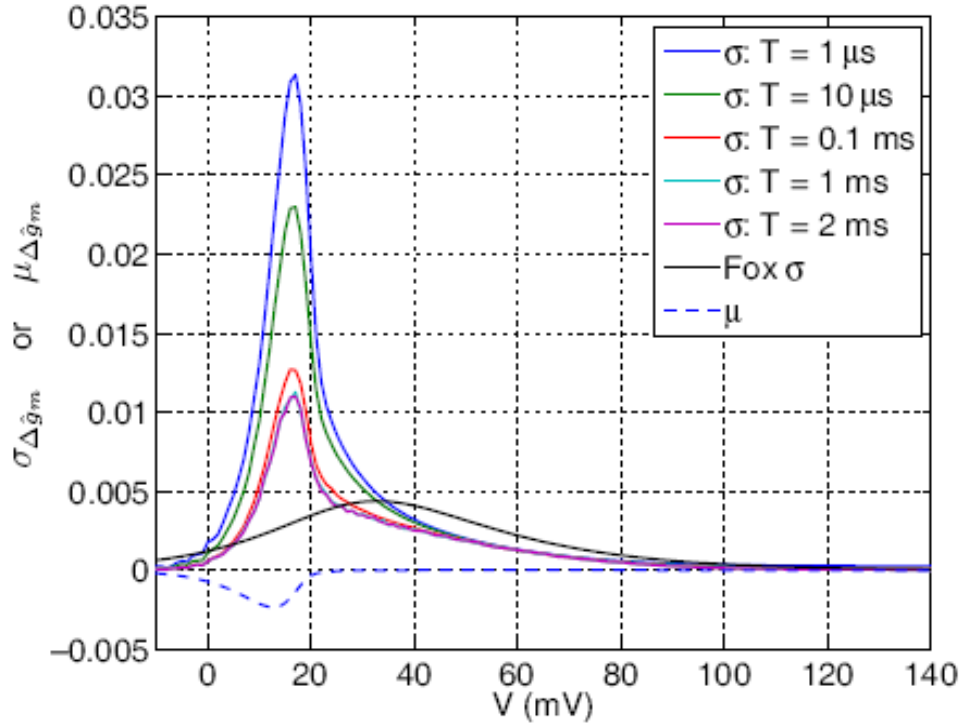

(from Bruce, *IEEE NE* 2007)

Fig. 4. Activation statistics for 1,000 sodium channels: standard deviation and mean of $\Delta\hat{g}_m$ as a function the relative transmembrane potential V. Standard deviations are calculated for values of $\Delta\hat{g}_m$ averaged over contiguous time windows of duration T, as indicated in the figure legend. The theoretical standard deviation versus membrane potential relationship given by (8) is shown for comparison.

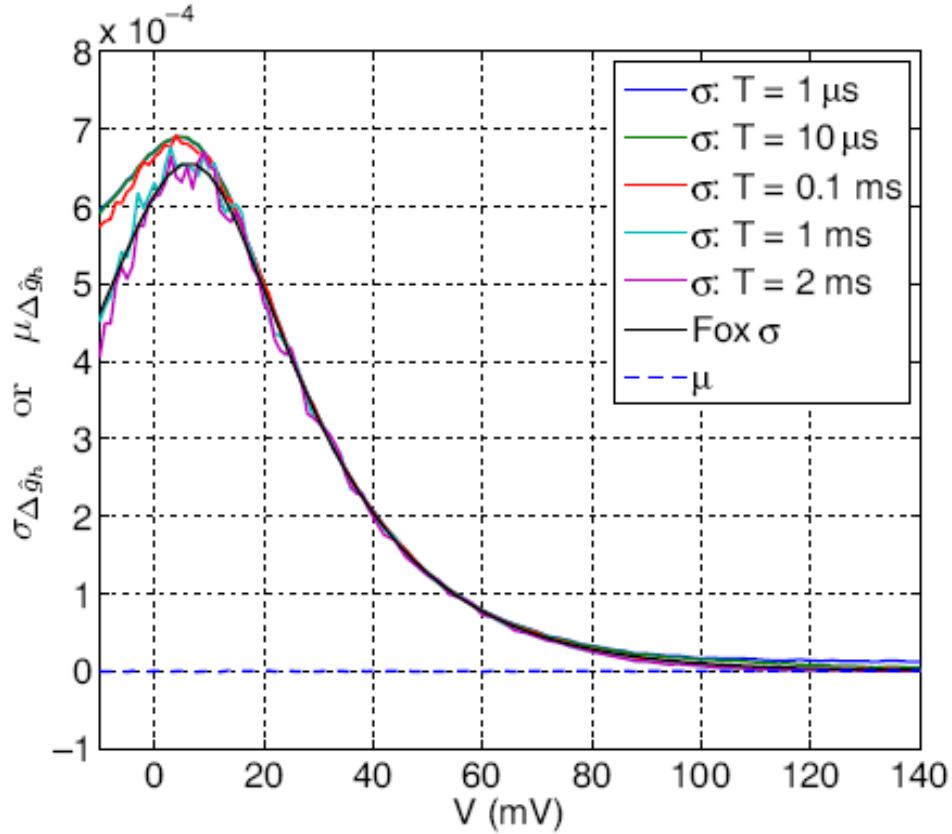

(from Bruce, *IEEE NE* 2007)

Fig. 5. Inactivation statistics for 1,000 sodium channels: standard deviation and mean of $\Delta\hat{g}_h$ as a function the relative transmembrane potential V. Standard deviations are calculated for values of $\Delta\hat{g}_h$ averaged over contiguous time windows of duration T, as indicated in the figure legend. The theoretical standard deviation versus membrane potential relationship given by (8) is shown for comparison.

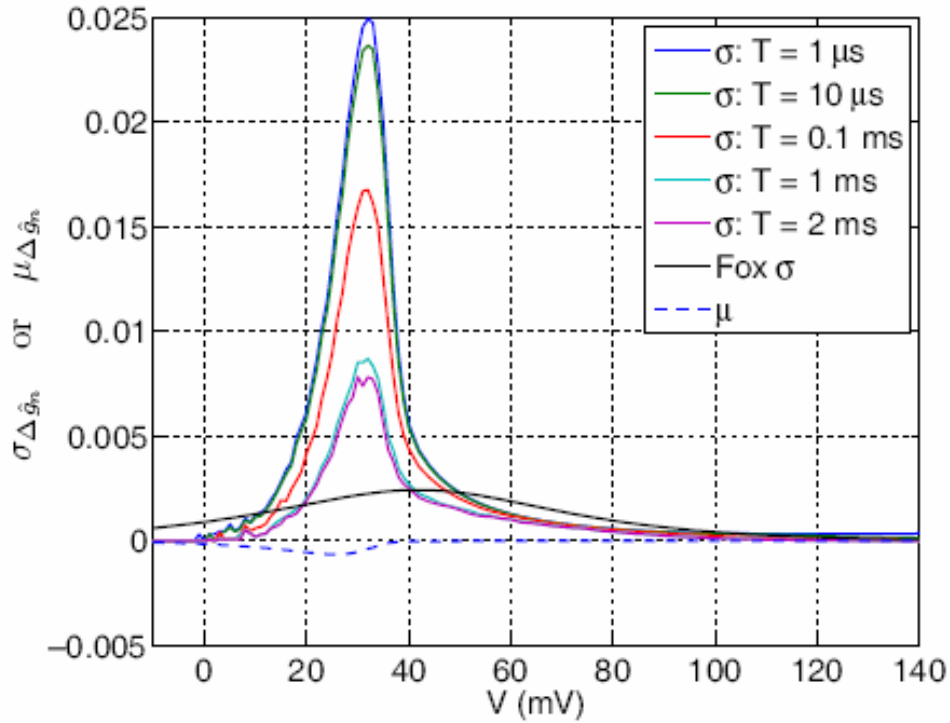

(from Bruce, *IEEE NE* 2007)

Fig. 6. Activation statistics for 333 potassium channels: standard deviation and mean of $\Delta\hat{g}_n$ as a function the relative transmembrane potential V. Standard deviations are calculated for values of $\Delta\hat{g}_n$ averaged over contiguous time windows of duration T, as indicated in the figure legend. The theoretical standard deviation versus membrane potential relationship given by (8) is shown for comparison.